



Expression of retinoic acid-related orphan receptor alpha and its responsive genes in human endometrium regulated by cholesterol sulfate

Fumiko Zenri^a, Hisahiko Hiroi^a, Mikio Momoeda^{a,b,*}, Ryo Tsutsumi^a, Yumi Hosokawa^a, Minako Koizumi^a, Hanako Nakae^a, Yutaka Osuga^a, Tetsu Yano^a, Yuji Taketani^a

^a Department of Obstetrics and Gynecology, Faculty of Medicine, The University of Tokyo, Japan

^b Department of Integrated Women's Health, St. Luke's International Hospital, Japan

ARTICLE INFO

Article history:

Received 14 May 2011

Received in revised form

27 September 2011

Accepted 8 October 2011

Keywords:

Cholesterol sulfate

Retinoic acid-related orphan receptor alpha

(RORA)

NR1D1

ABSTRACT

Cholesterol sulfate (CS) is a major sterol sulfate in human plasma that is detected in the uterine endometrium. CS plays a role in steroidogenesis, cellular membrane stabilization, and regulation of the skin barrier. We previously reported that CS increased in rabbit endometrium during the implantation period. Recently, CS has been reported to be a ligand of retinoic acid receptor-related orphan receptor alpha (RORA). NR1D1 is one of the genes regulated by RORA. In the present study, we investigated the regulation of RORA and NR1D1 by CS in human endometrium. We determined the association–dissociation curves for the interaction of CS with RORA and the kinetic rates by surface plasmon resonance. Immunohistochemical staining and *in situ* hybridization revealed that RORA and NR1D1 were expressed in human endometrial stromal and epithelial cells. CS treatment significantly induced the mRNA expression of RORA and NR1D1 mRNA in ESCs. The results of a luciferase assay showed that RORA significantly activated the human NR1D1 promoter regardless of CS. Our results suggest that CS regulates the expression of RORA responsive genes in human endometrial cells but not as a ligand for RORA.

© 2011 Elsevier Ltd. All rights reserved.

1. Introduction

The primary functions of uterine endometrial cells are receiving fertilized eggs and offering an environment for embryonic growth during the implantation window. In the human endometrium, endometrial epithelial cells structurally and functionally change and secrete glycoproteins and specific proteins. Subsequently, endometrial tissue changes dramatically during decidualization. It has been proposed that sulfatide is the only glycolipid that changes in rabbit endometrium throughout the menstrual cycle. Specifically, the level of acidic glycosphingolipids dramatically increases during the secretory phase [1–3], whereas the level of cholesterol sulfate (CS) increases in rabbit endometrium during the implantation window and steroid sulfatase activity concomitantly decreases [1,3]. In human endometrium, cholesterol sulfotransferase 2B1b (SULT2B1b), an enzyme involved in CS synthesis, is increased in human endometrium during the implantation period [4]. CS is a major sterol sulfate in human plasma that is detectable in the endometrial cells of the uterus, lungs, skin, hair, adrenal glands, and

nails. CS plays a role in cellular membrane stabilization, regulation of the skin barrier, and steroidogenesis [5–7]. Recently, we reported the inhibitory effect of proteases on CS in human endometrium [8,9]. CS was demonstrated to be a natural ligand of the retinoic acid receptor-related orphan receptor alpha (RORA) [10,11]. Mass spectrometry analysis led to the prediction that CS should have a higher affinity for RORA than cholesterol [10], and X-ray crystal structure analysis revealed the stable binding of CS with the ligand-binding domain of RORA [11].

RORA is a member of the nuclear hormone receptor super family ($\alpha 1$, $\alpha 2$, $\alpha 3$, and $\alpha 4$) [12]; members of this super family differ in their N-terminal domains and display distinct DNA recognition and transactivation properties [13]. RORA binds in a monomer fashion to response elements composed of 6-bp A/T-rich sequences preceding a site core motif AGGTCA in the promoter of target genes [13,14]. RORA has been implicated in numerous age-related phenotypes, including atherosclerosis, cerebellar atrophy, immunodeficiency, and bone metabolism [15]. RORA is a functional component of the cell-autonomous core circadian clock [16], and RORA and CS activate hypoxia-inducible factor (HIF)-1 α [17]. The HIF pathway and HIF-regulated genes regulate uteroplacental angiogenesis, endometrial epithelial cell functions, and peri-implantation uterine receptivity [18].

The expression of NR1D1 mRNA is regulated by RORA. The Rev-erb is a subfamily of orphan nuclear receptors that consists of

* Corresponding author at: Department of Integrated Women's Health, St. Luke's International Hospital, 9-1 Akashi-cho, Chuo-ku, Tokyo 104-8560, Japan. Tel.: +81 3 3541 5151; fax: +81 3 5550 2605.

E-mail address: momoeda-ky@umin.ac.jp (M. Momoeda).

two different genes: NR1D1 (also referred to as ear1 or Rev-erba) and NR1D2 (also referred to as ear1 β or Rev-erb β) [19]. RORA1 especially binds to the Rev-Dr2 site in the NR1D1 gene promoter, which includes RORA response elements [20]. NR1D1 is widely expressed in the muscle, liver, and brain [20–22] but repressed during myocyte differentiation [22]. NR1D1 is also related to circadian rhythms [23,24], and a functional NR1D1-binding site has been identified in the NR1D1 gene promoter. NR1D1 was shown to negatively regulate the activity of its own promoter through this site [25].

In the present study, to elucidate the function of CS in endometrium, we determined the localization and regulation of RORA and one of its response genes, NR1D1, in human endometrium. Because NR1D1 is a RORA response gene, we examined the regulation of NR1D1 gene expression as a marker of RORA function in human endometrium.

2. Materials and methods

2.1. Collection of samples

Endometrial tissues were obtained from women undergoing a hysterectomy for benign gynecological conditions. In total, 60 women aged 40–48 years were recruited in the present study. All women had regular menstrual cycles, and none had received hormonal treatment for at least 3 months before surgery. The tissues were collected under sterile conditions and processed for primary cell culture. The phases of the menstrual cycles were determined and classified as early, mid, and late, proliferative phase, as well as secretory phases, according to the last and next menstrual period, basal body temperature, ultrasound findings on the endometrium and ovarian follicles, and standard histological criteria [26]. The experimental procedures were approved by the Institutional Review Board of the University of Tokyo, and signed informed consent for use of the samples was obtained from each woman.

2.2. Isolation and culture of human endometrial stromal and epithelial cells

The techniques used for isolation and culture of human endometrial stromal cells (ESCs) and epithelial cells (EECs) were previously described in the literature [4,27,28]. Fresh endometrial biopsy specimens collected in a sterile medium were rinsed to remove blood cells. The tissues were minced into small pieces and incubated in Dulbecco's modified Eagle medium: Nutrient Mixture F-12 (DMEM/F12) (Gibco, Long Island, NY, USA), containing 0.25% type-I collagenase (Sigma, Tokyo, Japan) and 15 U/ml deoxyribonuclease I (Invitrogen, Carlsbad, CA, USA), for 2 h at 37 °C. The resultant dispersed endometrial cells were separated by filtration through a 40- μ m nylon cell strainer (Becton Dickinson, Lincoln Park, NJ). The endometrial epithelial glands that remained intact were retained by the strainer, whereas the dispersed ESCs passed through the strainer into the filtrate. The ESCs in the filtrate were collected by centrifugation and resuspended in DMEM/F12 containing 10% charcoal-stripped fetal bovine serum (FBS, Hyclone, Logan, UT, USA), 100 U/ml penicillin, 0.1 mg/ml streptomycin, and 0.25 μ g/ml amphotericin B (Sigma). The ESCs were plated on 100-mm culture plates (Becton Dickinson) and kept at 37 °C in a humidified 5% CO₂/95% air atmosphere. At the first passage, the cells were plated into 6-well culture plates at a density of 5×10^5 cells/well (Becton Dickinson) for the reverse transcription-polymerase chain reaction (RT-PCR), quantitative RT-PCR, and Western blotting. EECs were collected by backwashing the strainer with DMEM/F12, placed in a 100-mm plate and incubated at 37 °C for 30 min to allow contaminated stromal cells to attach

to the plate wall. The unattached epithelial cells were recovered and cultured in the medium as described above at a density of 2×10^5 cells/well in 12-well culture plates (Becton Dickinson, Tokyo, Japan). The purity of both the stromal and epithelial cell preparations was more than 95%, as judged by positive cellular staining for vimentin or cytokeratin, and negative staining for CD45 (which identifies leukocytes) [28,29].

2.3. CS treatment of the cells

When the ESCs and EECs approached confluence, the complete medium was removed and replaced with fresh media and antibiotics. The cells were treated with 10 μ M CS [30] in the presence of 0.2% dimethyl sulfoxide (DMSO) (Sigma) for 1, 3, 6, 12, and 24 h. Control cells were treated with 0.2% DMSO for 3 h.

2.4. RORA protein expression and purification

Transfection was performed with FuGENE6 following the manufacturer's guidelines (Roche Applied Science, Indianapolis, IN, USA). Briefly, COS1 cells were plated in 100-mm culture plates (Becton Dickinson, Tokyo, Japan) kept at 37 °C in a humidified 5% CO₂/95% air atmosphere and grown overnight to achieve 70–80% confluence. The coding regions of RORA were ligated into the pcDNA4/HisMax-TOPO vector (RORAWt) (Invitrogen, Tokyo, Japan). The transfection complex was directly added to the wells in the presence of nonserum-containing medium. After 48 h, the transfected cells were washed with PBS and collected by centrifugation at 1000 \times g for 5 min. The His-tagged proteins were purified using Ni-NTA magnetic agarose beads according to the manufacturer's instructions (Qiagen, Tokyo, Japan). The elution buffer was replaced with distilled water for exchange with a HiTrapTM desalting column (GE Healthcare, Tokyo, Japan).

2.5. Surface plasmon resonance (SPR) analysis and analyte recovery

All experiments were performed at 25 °C using the Biacore 3000 SPR sensor (Biacore, Tokyo, Japan) with control software version 4.0 and a CM5 (carboxymethylated dextran surface) sensor chip. The chip surface was first activated following a standard N-hydroxysuccinimide (NHS) and carbodiimide (EDC) Biacore protocol. RORA proteins were immobilized via amine groups in all four of the available flow cells. HBS-P buffer (0.01 M HEPES, pH 7.4, 0.15 M NaCl, 0.005% surfactant-P20) (Biacore) was used as the running buffer. RORA at a concentration of 0.1 mg/ml in 10 mM potassium-phosphate buffer, pH 7.4, was then injected for 10 min followed by a 7-min injection of 1 M ethanolamine, pH 8.5, to inactivate the residual active groups. Finally, the surface was treated with 10 half-minute pulses of 50 mM NaOH to remove non-covalently bound RORA. Typically, about 15,000 RU of RORA was immobilized per flow cell 1 and flow cell 2 (Fc1 and Fc2). Fc1 and Fc2 were used for analysis after capture and recovery. The flow system was then washed and rinsed with HBS-P buffer. Fc1, which was the control, was rinsed with 5% DMSO, 0.05% surfactant-P20, and HBS-P buffer. Fc2 was rinsed with CS (20 μ M, 10 μ M, 5 μ M, 2.5 μ M, and 1.25 μ M), 5% DMSO, 0.05% surfactant-P20, and HBS-P buffer. Finally, the flow cells were rinsed with 5% DMSO, 0.05% surfactant-P20, and HBS-P buffer. The bound material was eluted with 50% DMSO and HBS-P buffer (used as the running buffer). Dissociation constants were derived by fitting the data into a 1:1 Langmuir binding model with BIAevaluation 3.0 software (Biacore). The apparent association (k_a) and dissociation rate constants (k_d) were evaluated from the differential binding curves (Fc2–Fc1). Two independent sets of measurements were used to calculate the rate constants. The affinity constant K_D was calculated by the equation $K_D = k_d/k_a$.

SPR response values are expressed in resonance units (RU). One RU represents a change of 0.0001° in the angle of the intensity minimum. For most proteins, this is roughly equivalent to a change in concentration of approximately 1 pg/mm^2 on the sensor surface.

2.6. RNA extraction, cDNA synthesis and RT-PCR

Total RNA was extracted individually from the endometrial tissue, ESCs, and EECs using an RNeasy minikit (Qiagen, Hilden, Germany). One microgram of total RNA was reverse transcribed in a 20- μl volume using ReverTraAce- α (TOYOBO, Tokyo, Japan) according to the manufacturer's instructions. PCR was performed using ReverTra Dash (TOYOBO) according to the manufacturer's instructions. The DNA sequences of the RORA1 and NR1D1 primers were previously described [16,31]. RORA1 primers (sense, 5'-GTCAGCAGCTTCTACCTGGAC-3'; antisense, 5'-ATGCGCACAATGTCTGGGTA-3') were designed to amplify a 482-bp fragment. NR1D1 primers (sense, 5'-ATCCCGACAGTCTTGTCGT-3'; antisense, 5'-CTTTTGCCGAGCCTTTC-3') were designed to amplify a 419-bp fragment. β -Actin and G3PDH were used as internal controls. Primers for β -actin (sense, 5'-GATGACCCAGATCATGTTTGA-3'; antisense, 5'-CGGATGTCAACGTCACTTCATG-3') were designed to amplify the 517-bp fragments. Primers for G3PDH (sense, 5'-TCACCATCTTCCAGGAGCGA-3'; antisense, 5'-CACAATGCCGAAGTGGCTGT-3') were designed to amplify the 293-bp fragments.

The PCR conditions for amplification of RORA1 and NR1D1 were 30 cycles at 94°C for 10 s, 59.8°C for 2 s, and 74°C for 30 s. The PCR conditions for amplification of β -actin and G3PDH were 30 cycles at 94°C for 10 s, 60°C for 2 s, and 74°C for 30 s. PCR products were analyzed by 2% agarose gel electrophoresis with ethidium bromide. Each PCR product was purified with a QIAEX II gel extraction kit (Qiagen, Hilden, Germany) and subcloned into pCR2.1-TOPO vector with TOPO TA expression kit (Invitrogen, USA) to confirm sequences using an ABI PRISM 310 genetic analyzer (Applied Biosystems, Foster City, CA, USA).

2.7. Real-time quantitative PCR

To assess RORA1 and NR1D1 mRNA expression, real-time quantitative PCR and data analysis were performed using LightCycler (Roche Diagnostic GmbH, Mannheim, Germany) according to the manufacturer's instructions. Real-time quantitative PCR was performed using Lithos qPCR Master Mix Hot Start (Eurogentec, Tokyo, Japan) according to the manufacturer's instructions. The loaded amount of RORA1 and NR1D1 mRNA were normalized to β -actin mRNA as an internal control. The primers for RORA1, NR1D1, and β -actin were the same as those used for RT-PCR. The PCR conditions of RORA1 and NR1D1 were 30 cycles at 95°C for 15 s, 64°C for 8 s, and 72°C for 9 s. The β -actin conditions were 30 cycles at 95°C for 15 s, 64°C for 8 s, and 72°C for 25 s.

2.8. Western blotting

Cells were washed twice in PBS and then scraped into PBS containing protease inhibitors. To prepare whole-cell extracts, cells were resuspended in lysis buffer (PBS, 1% Nonidet P-40, 1 mM EDTA) containing the Complete Protease Inhibitor Cocktail (Roche). The samples were centrifuged ($12,000 \times g$) for 15 min at 4°C before supernatant was transferred to a new tube as whole-cell extracts. Nuclear extracts were prepared as described below. After adding Nonidet P-40 (final concentration at 0.625%) (WAKO, Tokyo, Japan), the cells were resuspended in buffer (10 mM KCl, 0.1 mM EDTA, 0.1 mM EGTA, 1 mM dithiothreitol, 10 mM HEPES, pH 7.9) containing protease inhibitors for 15 min on ice. After centrifugation ($12,000 \times g$) for 15 min at 4°C , the supernatants were removed, and the pellets (nuclear fraction) were resuspended in buffer (400 mM

NaCl, 1 mM EDTA, 1 mM EGTA, 1 mM dithiothreitol, 20 mM HEPES, pH 7.9) containing protease inhibitors and incubated for 15 min on ice. The samples were then centrifuged ($12,000 \times g$) for 15 min at 4°C , the nuclear protein extracts were collected, and the protein concentrations were determined with Bio-Rad Protein Assay reagents (Bio-Rad Laboratories, Inc., Hercules, CA, USA). Whole-cell extracts and nuclear extracts (8 μg of each sample) were used for Western blot analysis. Proteins were loaded onto 10% SDS-PAGE gels and then transferred to Immobilon polyvinylidene difluoride membranes (Millipore Corp, Bedford, MA, USA). Western blot analysis was conducted using the following primary antibodies: anti-RORA (1:1000; Affinity BioReagents, Rockford, IL, USA), anti-G3PDH (1:2000; Santa Cruz Biotechnology, Santa Cruz, CA, USA), anti-NR1D1 (1:100; Perseus Proteomics, Tokyo, Japan), and anti- β -actin (1:3000; Sigma). RORA immunoreactive bands were visualized with horseradish peroxidase-conjugated anti-rabbit IgG (1:3000; Santa Cruz Biotechnology). G3PDH immunoreactive bands were visualized with horseradish peroxidase-conjugated anti-goat IgG (1:2000; Santa Cruz Biotechnology). NR1D1 and β -actin immunoreactive bands were visualized with horseradish peroxidase-conjugated anti-mouse IgG (1:3000; Santa Cruz Biotechnology). The ECL Plus Western blotting system was used to detect antibody protein complexes (Amersham Biosciences).

2.9. Immunohistochemical staining

Sections were treated with 3% hydrogen peroxide for 30 min to eliminate endogenous peroxidase. After blocking with 1.5% mouse serum, the sections were stained first with RORA polyclonal antibody (1/25), which was the same as for Western blotting, using a histofine SAB-PO MULT kit (Nichirei Corporation, Tokyo, Japan) overnight at 4°C . Control slides were incubated with nonimmune rabbit IgG, the concentration of which was adjusted to that of the primary antibody. The sections were then incubated with biotinylated horse antirabbit IgG followed by avidin-peroxidase using the ABC kit (Nichirei Corporation, Tokyo, Japan). The chromogenic reaction was carried out with diaminobenzidine (Nichirei Corporation, Tokyo, Japan). All sections were counterstained with hematoxylin. We performed immunohistochemical staining with at least three samples during each menstrual phase. Assessments of immunostaining were based on agreement among three

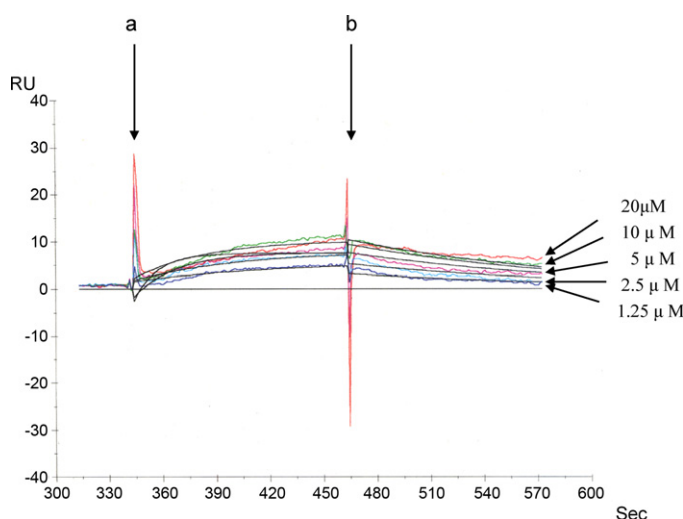


Fig. 1. The CS-RORA association and dissociation curve. Sensorgram with different concentrations of CS and fitted curve based on the bivalent analyte model. Binding to CS layers was tested at 20 μM , 10 μM , 5 μM , 2.5 μM , and 1.25 μM . (a) Start of CS injection and (b) end of CS injection. The data shown are representative of three different samples.

independent observers who were blind to the phases of the menstrual cycle at which the specimens were collected.

2.10. *In situ* hybridization

For preparation of the digoxigenin (DIG)-labeled RNA probe for NR1D1, the 419-bp fragment of human NR1D1 complementary DNA, obtained by RT-PCR with the primers described, was subcloned into the appropriate restriction site of the PCR II-TOPO vector (Invitrogen, Carlsbad, CA, USA). After linearization of the plasmid with an appropriate restriction enzyme, the linearized

vectors were used as templates for the synthesis of DIG-labeled RNA probes using SP6 or T7 RNA polymerase. *In situ* hybridization was performed using an ISHR starting kit (Nippon Gene, Toyama, Japan) as described previously [32]. Briefly, tissue collected for *in situ* hybridization was fixed by immersing in 10% neutral buffered saline overnight at 4°C before routine paraffin embedding. The paraffin-embedded specimens were sliced to sections with a thickness of 5 µm. These sections were mounted on poly-L-lysine-treated slides, deparaffinized, and rehydrated. They were further digested with 5 mg/ml proteinase K for 10 min at room temperature, treated with acetic anhydride, and then subjected

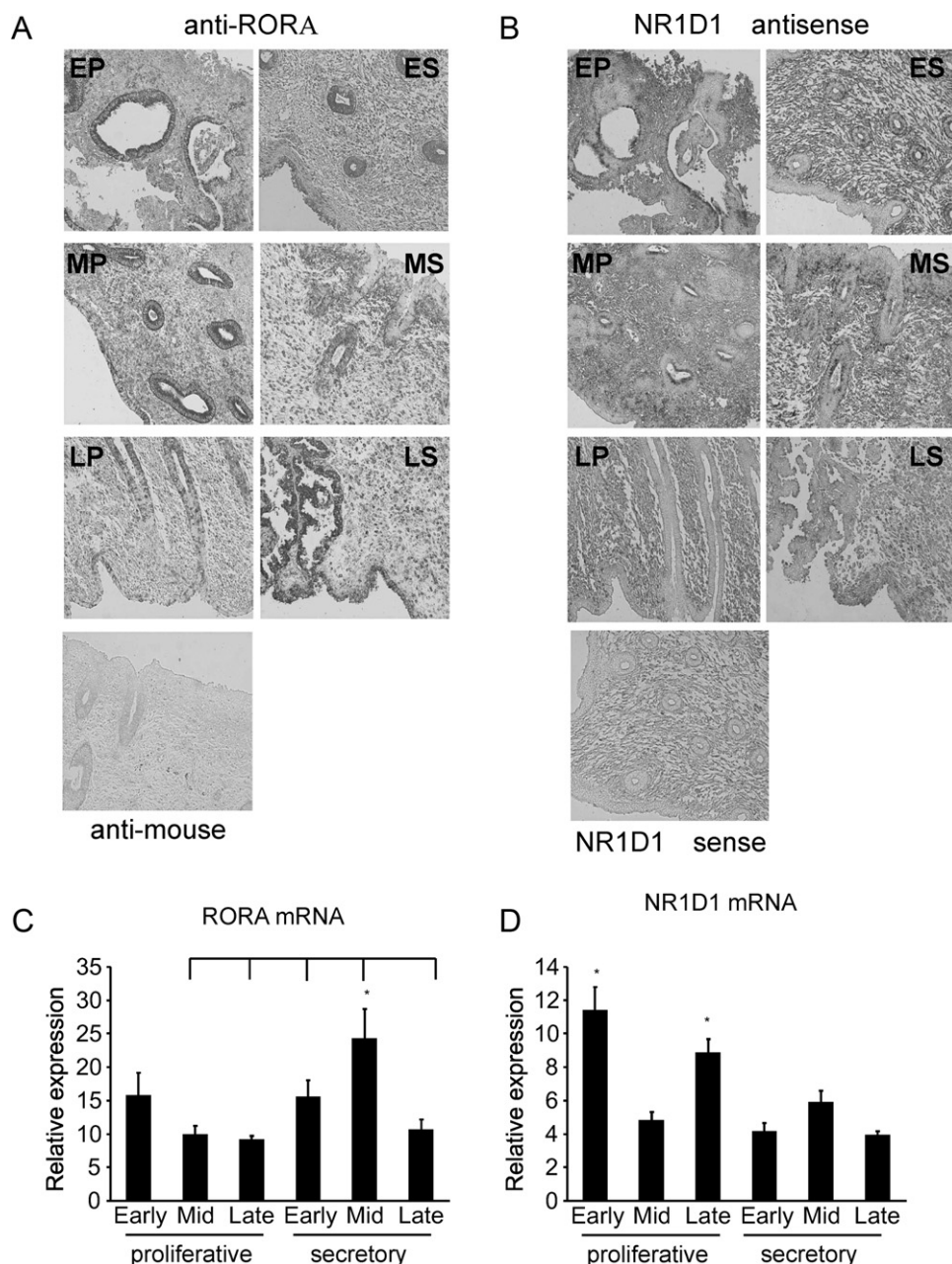


Fig. 2. Expression and localization of RORA and NR1D1 gene product in human endometrium. (A) Immunohistochemical staining for RORA in human endometrium throughout the menstrual cycle. (B) *In situ* hybridization of NR1D1 in human endometrium throughout the menstrual cycle. EP, early proliferative phase; MP, mid-proliferative phase; LP, late proliferative phase; ES, early secretory phase; MS, mid-secretory phase; LS, late secretory phase. Control slide for RORA was incubated with nonimmune mouse IgG. Magnification, 100×. (C) Expression of RORA mRNA in the human endometrium throughout the menstrual cycle estimated by real-time quantitative RT-PCR. (D) Expression of NR1D1 mRNA in the human endometrium throughout the menstrual cycle estimated by real-time quantitative RT-PCR. Endometrial tissues were obtained from 36 women in EP, early proliferative phase, $n=4$; MP, mid-proliferative phase, $n=7$; LP, late proliferative phase, $n=6$; ES, early secretory phase, $n=9$; MS, mid-secretory phase, $n=6$; LS, late secretory phase, $n=4$. Results were normalized for the amount of β -actin. Mean \pm SEM within a panel with different superscripts are statistically different ($P<0.05$).

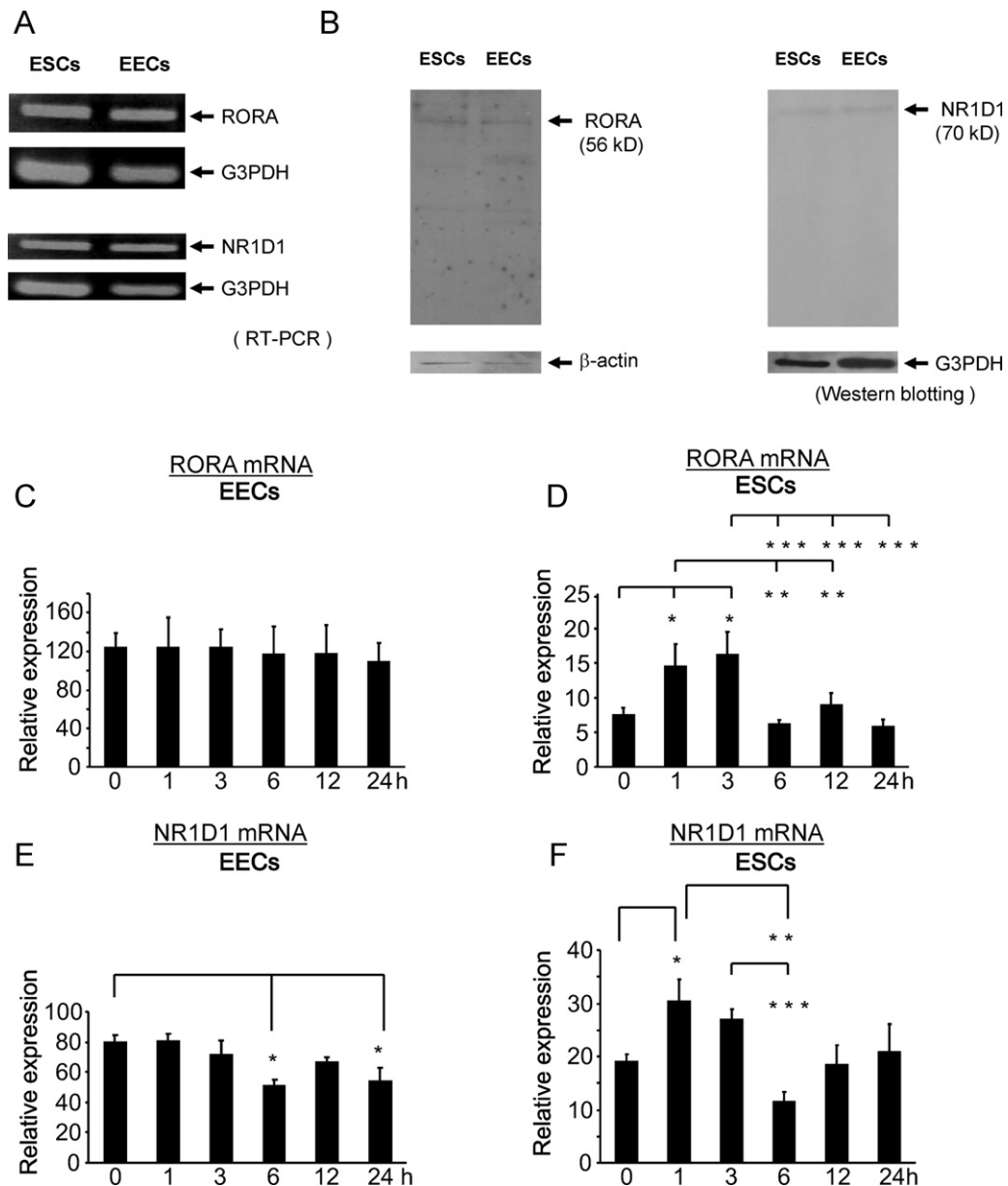


Fig. 3. Expression of RORA and NR1D1 gene product in cultured human endometrial cells. (A) Expression of RORA and NR1D1 mRNA in cultured human endometrial stromal cells (ESCs) and epithelial cells (EECs), as detected by standard RT-PCR. The internal control was G3PDH. The data shown are representative of three different samples. (B) Expression of the RORA and NR1D1 protein was examined by Western blotting in ESCs and EECs. The internal control for RORA was β -actin, and that of NR1D1 was G3PDH. The results are representative of four independent experiments using samples from different women. (C) Expression of RORA mRNA in cultured human EECs after treatment with cholesterol sulfate (CS) estimated by real-time quantitative RT-PCR. The data shown are representative of four independent samples. (D) Expression of RORA mRNA in cultured human ESCs after treatment with CS estimated by real-time quantitative RT-PCR. The data shown are representative of four independent samples. (E) Expression of NR1D1 mRNA in cultured human EECs after treatment with cholesterol sulfate (CS) estimated by real-time quantitative RT-PCR. The data shown are representative of five independent samples. (F) Expression of NR1D1 mRNA in cultured human ESCs after treatment with CS estimated by real-time quantitative RT-PCR. The data shown are representative of five independent samples. Results were normalized to the amount of β -actin. Mean \pm SEM within a panel with different superscripts are statistically different ($P < 0.05$).

to treatment with pre-hybridization solution in ISHR starting kit for 30 min at 42 °C. Hybridization was performed by applying the diluted probe to each slide section. Each section was incubated in a humidified chamber overnight at 42 °C. Slides were washed and then treated with RNase for 30 min at 37 °C. After being blocked with blocking reagent in ISHR starting kit, the sections were incubated with anti-DIG, alkaline phosphatase-conjugated antibody (1:500, Roche) for 1 h at room temperature. Color development was carried out by overlaying the sections with nitroblue tetrazolium/5-bromo-4-chloro-3-indolyl phosphate (Roche) and incubating in a humidified container in the dark for 12 h. Sense probe hybridization was used as a control for background level. We performed *in situ*

hybridization with at least three samples during each menstrual phase.

2.11. Plasmid construction, cell culture and luciferase assay

The coding regions of RORA were subcloned into the pcDNA4/HisMax-TOPO vector (RORAWt) (Invitrogen, Tokyo, Japan). Human NR1D1 promoter including RORA response elements (RORE) (−66/+6) was amplified by PCR (sense, 5′-CCGCTC-GAGATCCCGACAGTCTTGTCGT-3′; antisense, 5′-GGAAGATCTCTT-TTGCCCGAGCCTTTC-3′) and subcloned into the pGL3-Basic vector (Rev-Dr) (Invitrogen). The sequence of PCR product was confirmed

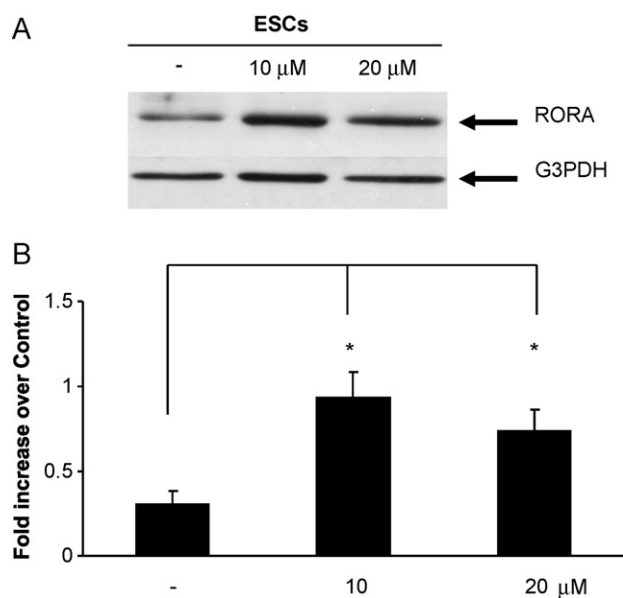


Fig. 4. Expression of RORA protein in cultured human endometrial stromal cells (ESCs). (A) Expression of RORA protein was examined by Western blotting in cultured endometrial stromal cells (ESCs) after treatment with cholesterol sulfate (CS) at 10 μ M and 20 μ M for 3 h. The results are representative of four individual experiments using samples from different women. (B) Scanned data of three independent Western blotting analyses. Results were normalized to the amount of G3PDH protein and presented as the mean \pm SEM ($P < 0.05$).

by ABI PRISM 310 genetic analyzer (Applied Biosystems). Generally, the dominant negative mutant of RORA (ROR D-mt) is the N-terminal fragment of RORA (1–705), which lacks the ligand-binding domain. The N-terminal fragment of RORA was subcloned into pcDNA4/HisMax-TOPO vector. Their identities were confirmed using the ABI PRISM 310 genetic analyzer. COS1 cells were maintained in standard conditions DMEM supplemented with 10% FBS at 37°C in a humidified 5% CO₂/95% air atmosphere. Medium was changed every 3 days. Cells were seeded in 12-well plates at a density of 1×10^5 and incubated at 37°C for 12 h to achieve 70–80% confluence prior to transfection. Cells were transfected using transfection reagent FuGENE6 with the reporter vector (Rev-Dr, 200 ng/well), expression vector (RORAWt or ROR D-mt, 200 ng/well), the control vector (pRL-SV40, 100 ng/well) (Invitrogen), and the control plasmid vector (pcDNA4/HisMax-TOPO vector) (Invitrogen). At the end of the experiments, the cells were washed once with ice-cold 0.15 M NaCl, 0.01 M sodium phosphate buffer, pH 7.2. Luciferase assays were performed using the Dual-Luciferase Reporter Assay System (TOYO Tokyo, Japan), in which Renilla luciferase plasmids were co-transfected as control plasmids to standardize transcription efficiency. All transfection experiments were performed at least three times.

2.12. Statistical analysis

The results are presented as the mean \pm SEM. The analysis was conducted by one-way analysis of variance (ANOVA) with a post hoc analysis (Fisher's protected least significance). Statistical significance was accepted at $P < 0.05$.

3. Results

3.1. The interaction of CS with RORA

The association–dissociation curves for the interaction of CS with RORA are illustrated in Fig. 1. The k_a , k_d , and KD values are 7.01×10^3 (1/Ms), 7.62×10^{-3} (1/s), and 1.09×10^{-6} (M),

respectively. Fig. 1 indicates that cholesterol did not interact with RORA under the same conditions.

3.2. The expression of RORA and NR1D1 in human endometrium

The RORA protein was localized in human endometrial stromal and epithelial cells throughout all phases of the human menstrual cycle (Fig. 2A), and no change was detected in the localization of the RORA protein throughout the entire cycle. The *in situ* hybridization (Fig. 2B) showed that NR1D1 mRNA was expressed during all phases of the menstrual cycle in glandular and luminal epithelial cells and in stromal cells during the early proliferative phase of the cycle. During the mid-proliferative and early and mid-secretory phases of the menstrual cycle, NR1D1 mRNA was detected in both glandular epithelial cells and stromal cells. During the late proliferative and late secretory phases, NR1D1 mRNA was detected in stromal cells (Fig. 2B). Although we tried to perform immunohistochemistry with several anti-NR1D1 antibodies, only severe non-specific signal was detected. Real-time quantitative PCR analysis showed that RORA (Fig. 2C) and NR1D1 (Fig. 2D) were expressed in endometrial tissues throughout the human menstrual cycle. The expression of RORA mRNA significantly increased during the mid-secretory phase (Fig. 2C), and that of NR1D1 increased during the early and late proliferative phases of the human menstrual cycle (Fig. 2D).

3.3. The regulation of RORA and NR1D1 mRNA expression by CS

RORA and NR1D1 mRNA expression in EECs and ESCs was detected by standard RT-PCR analysis (Fig. 3A). The expression of RORA and NR1D1 proteins in EECs and ESCs was detected as bands at 56 kDa and 66.8 kDa in EECs and ESCs by Western blotting (Fig. 3B). The expression of RORA mRNA did not change in EECs after treatment with 10 μ M CS (Fig. 3C) but increased significantly in ESCs 1 and 3 h after treatment with 10 μ M CS (Fig. 3D). The expression of NR1D1 mRNA decreased in EECs 6 h after treatment with 10 μ M CS (Fig. 3E) and increased in ESCs 1 h after treatment with 10 μ M CS (Fig. 3F). The amount of RORA protein was significantly higher in ESCs 3 h after treatment with 10 and 20 μ M CS, but there was no significant difference between the 10 and 20 μ M treatments (Fig. 4).

3.4. The transcriptional activity of RORA

RORAWt significantly activated the human NR1D1 promoter. Although there was no ligand-binding domain in the ROR D-mt, the human NR1D1 promoter was also significantly activated. There was no change in the activation of NR1D1 promoter regardless of CS (Fig. 5).

4. Discussion

For the first time, we demonstrated the expression of RORA and NR1D1 in human endometrium, cultured EECs, and cultured ESCs. RORA is widely expressed in peripheral tissues, especially in the liver and muscle [10,33], and it has many roles including myocyte differentiation [34], lipid metabolism [35,36], inflammation control [37,38], and the negative regulation of ischemia-induced angiogenesis [39]. It was recently reported that HIF-1 α expression is regulated by CS via RORA [17]. The HIF pathway and HIF-regulated genes are associated with angiogenesis [18]. NR1D1 is known to have similar functions as RORA, and both RORA and NR1D1 regulate the expression of the plasminogen activator inhibitor type-1 (PAI-1) gene [40]. Increased uterine vascular permeability and angiogenesis are important for implantation. These findings

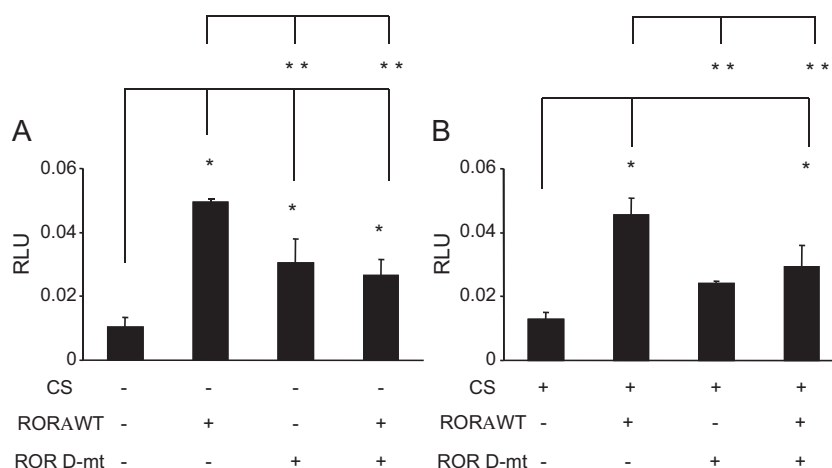


Fig. 5. The luciferase assay with RORA wild type and dominant negative mutant of RORA. (A) Transcriptional activity of RORA wild type (RORAWt) and dominant negative mutant of RORA (ROR D-mt) via human NR1D1 promoter by luciferase assay without CS. (B) Transcriptional activity of RORAWt and ROR D-mt via human NR1D1 promoter by luciferase assay with 10 μ M CS. RLU, relative light units. The data shown are representative of three independent experiments and presented as the mean \pm SEM ($P < 0.05$).

indicate that RORA and NR1D1 might regulate vascular formation in human endometrium.

We studied the expression and localization of RORA and NR1D1 in human endometrium (Fig. 2). It has been reported that NR1D1 exhibited significant rhythmicity in rat oviduct, suggesting that the developing embryo is subjected to rhythmic changes in the environment created by the oviduct [41]. It is possible that changes in the expression and localization of RORA and NR1D1 during the menstrual cycle might be related to the development of the embryo, which supports a role for RORA and NR1D1 expression in implantation within the human uterus. The change of RORA mRNA expression was almost same as NR1D1 mRNA expression in ESCs after treatment with CS, indicating that NR1D1 mRNA expression is regulated via RORA (Fig. 3). But Fig. 2 shows that NR1D1 mRNA expression was not parallel with RORA mRNA expression in human endometrium during menstrual cycle. One possible explanation is that the condition of cultured cells may differ from endometrium. It is possible that the other regulatory factors may act on in vivo NR1D1 transcription in human endometrium.

The expression of RORA mRNA and protein significantly increased 1 and 3 h after treatment with 10 μ M CS in ESCs (Figs. 3D and 4). We previously reported that CS increased during the implantation period in rabbit endometrium [1,3]. Also, in human endometrium, we recently revealed that cholesterol sulfotransferase 2B1b, an enzyme of CS synthesis, increased during the mid-secretory phase of the menstrual cycle [4]. In the present study, the amount of RORA mRNA increased during the mid-secretory phase (Fig. 2C). These results suggest that CS may regulate RORA expression in the human endometrium. RORA transcriptional activity can be modulated by changes in intracellular cholesterol levels or by mutation of residues involved in cholesterol binding [42]. Intracellular cholesterol in mammalian cells is determined by the uptake of serum low-density lipoprotein (LDL), which may also follow a circadian rhythm [43].

In the present study, we found that CS had a higher affinity for RORA than cholesterol (Fig. 1). Several lines of evidence indicate that CS is a natural ligand of RORA [10,11]. NR1D1 mRNA is regulated by RORA [20]. In the present study, we revealed that CS regulated NR1D1 transcription in ESCs (Fig. 3F). However, as shown by the results of the luciferase assay, CS did not function as a ligand for RORA (Fig. 5). Because of low efficiency of transfection and sample limitation, we did not use endometrial cells for the luciferase assay. The physiological condition of endometrial cells is different from COS1 cells. One possible explanation is that COS1 cells may

not contain cofactors necessary for RORA to act as receptor of CS. A second possible explanation is that CS increases RORA expression, which subsequently regulates NR1D1 in human endometrium.

In the present study, we show that CS regulates the expression of RORA responsive genes in human endometrial cells. This effect is exerted by up-regulation of RORA transcription but not by action as a ligand for RORA. Our results indicate that CS may regulate the expression of genes via the regulation of RORA expression in human endometrium. As mentioned above, the level of CS increases during the implantation window in endometrium. It is possible that CS may play an important role in the differentiation of the endometrium in preparation for implantation.

Acknowledgments

We would like to thank Osamu Tsutsumi, M.D., Ph.D. (Sanno Hospital, Tokyo), for guidance and insight and Emi Nose for technical assistance.

References

- [1] M. Momoeda, Y. Taketani, M. Mizuno, M. Iwamori, Y. Nagai, Characteristic expression of cholesterol sulfate in rabbit endometrium during the implantation period, *Biochem. Biophys. Res. Commun.* 178 (1991) 145–150.
- [2] K. Kubushiro, K. Kojima, M. Mikami, S. Nozawa, R. Iizuka, M. Iwamori, Y. Nagai, Menstrual cycle-associated alteration of sulfogalactosylceramide in human uterine endometrium: possible induction of glycolipid sulfation by sex steroid hormones, *Arch. Biochem. Biophys.* 268 (1989) 129–136.
- [3] M. Momoeda, Y. Cui, Y. Sawada, Y. Taketani, M. Mizuno, M. Iwamori, Pseudopregnancy-dependent accumulation of cholesterol sulfate due to up-regulation of cholesterol sulfotransferase and concurrent down-regulation of cholesterol sulfate sulfatase in the uterine endometria of rabbits, *J. Biochem.* 116 (1994) 657–662.
- [4] M. Koizumi, M. Momoeda, H. Hiroi, Y. Hosokawa, R. Tsutsumi, Y. Osuga, T. Yano, Y. Taketani, Expression and regulation of cholesterol sulfotransferase (SULT2B1b) in human endometrium, *Fertil. Steril.* 93 (2010) 1538–1544.
- [5] C.A. Strott, Y. Higashi, Cholesterol sulfate in human physiology: what's it all about? *J. Lipid Res.* 44 (2003) 1268–1278.
- [6] T. Sugawara, E. Nomura, N. Hoshi, Cholesterol sulphate affects production of steroid hormones by reducing steroidogenic acute regulatory protein level in adrenocortical cells, *J. Endocrinol.* 195 (2007) 451–458.
- [7] R. Tsutsumi, H. Hiroi, M. Momoeda, Y. Hosokawa, F. Nakazawa, M. Koizumi, T. Yano, O. Tsutsumi, Y. Taketani, Inhibitory effects of cholesterol sulfate on progesterone production in human granulosa-like tumor cell line, KGN, *Endocr. J.* 55 (2008) 575–581.
- [8] M. Koizumi, M. Momoeda, H. Hiroi, F. Nakazawa, H. Nakae, T. Ohno, T. Yano, Y. Taketani, Inhibition of proteases involved in embryo implantation by cholesterol sulfate, *Hum. Reprod.* 25 (2010) 192–197.
- [9] H. Nakae, H. Hiroi, M. Momoeda, M. Koizumi, M. Iwamori, Y. Taketani, Inhibition of cell invasion and protease activity by cholesterol sulfate, *Fertil. Steril.* 94 (2010) 2455–2457.

- [10] F. Bitsch, R. Aichholz, J. Kallen, S. Geisse, B. Fournier, J.M. Schlaeppi, Identification of natural ligands of retinoic acid receptor-related orphan receptor alpha ligand-binding domain expressed in Sf9 cells—a mass spectrometry approach, *Anal. Biochem.* 323 (2003) 139–149.
- [11] J. Kallen, J.M. Schlaeppi, F. Bitsch, I. Delhon, B. Fournier, Crystal structure of the human RORalpha Ligand binding domain in complex with cholesterol sulfate at 2.2 Å, *J. Biol. Chem.* 279 (2004) 14033–14038.
- [12] A.M. Jetten, S. Kurebayashi, E. Ueda, The ROR nuclear orphan receptor subfamily: critical regulators of multiple biological processes, *Prog. Nucleic Acid Res. Mol. Biol.* 69 (2001) 205–247.
- [13] V. Giguère, M. Tini, G. Flock, E. Ong, R.M. Evans, G. Otulakowski, Isoform-specific amino-terminal domains dictate DNA-binding properties of ROR alpha, a novel family of orphan hormone nuclear receptors, *Genes Dev.* 8 (1994) 538–553.
- [14] C. Carlberg, R. Hooft van Huijsduijnen, J.K. Staple, J.F. DeLamar, M. Becker-André, RZR8, a new family of retinoid-related orphan receptors that function as both monomers and homodimers, *Mol. Endocrinol.* 8 (1994) 757–770.
- [15] C.I. Jarvis, B. Staels, B. Brugg, Y. Lemaigre-Dubreuil, A. Tedgui, J. Mariani, Age-related phenotypes in the staggerer mouse expand the RORalpha nuclear receptor's role beyond the cerebellum, *Mol. Cell. Endocrinol.* 186 (2002) 1–5.
- [16] M. Akashi, T. Takumi, The orphan nuclear receptor RORalpha regulates circadian transcription of the mammalian core-clock Bmal1, *Nat. Struct. Mol. Biol.* 12 (2005) 441–448.
- [17] E.J. Kim, Y.G. Yoo, W.K. Yang, Y.S. Lim, T.Y. Na, I.K. Lee, M.O. Lee, Transcriptional activation of HIF-1 by RORalpha and its role in hypoxia signaling, *Arterioscler. Thromb. Vasc. Biol.* 28 (2008) 1796–1802.
- [18] R.D. Koos, A.A. Kazi, M.S. Roberson, J.M. Jones, New insight into the transcriptional regulation of vascular endothelial growth factor expression in the endometrium by estrogen and relaxin, *Ann. N. Y. Acad. Sci.* 1041 (2005) 233–247.
- [19] B.M. Forman, J. Chen, B. Blumberg, S.A. Kliewer, R. Henshaw, E.S. Ong, R.M. Evans, Cross-talk among ROR alpha 1 and the Rev-erb family of orphan nuclear receptors, *Mol. Endocrinol.* 8 (1994) 1253–1261.
- [20] E. Raspé, G. Mautino, C. Duval, C. Fontaine, H. Duez, O. Barbier, D. Monte, J. Fruchart, J.C. Fruchart, B. Staels, Transcriptional regulation of human Rev-erbalpha gene expression by the orphan nuclear receptor retinoic acid-related orphan receptor alpha, *J. Biol. Chem.* 277 (2002) 49275–49281.
- [21] P. Gervois, S. Chopin-Delannoy, A. Fadel, G. Dubois, V. Kosykh, J.C. Fruchart, J. Najib, V. Laudet, B. Staels, Fibrates increase human REV-ERBalpha expression in liver via a novel peroxisome proliferator-activated receptor response element, *Mol. Endocrinol.* 13 (1999) 400–409.
- [22] M. Downes, A.J. Carozzi, G.E. Muscat, Constitutive expression of the orphan receptor, Rev-erbA alpha, inhibits muscle differentiation and abrogates the expression of the myoD gene family, *Mol. Endocrinol.* 9 (1995) 1666–1678.
- [23] I.P. Torra, V. Tsubulsky, F. Delaunay, R. Saladin, V. Laudet, J.C. Fruchart, V. Kosykh, B. Staels, Circadian and glucocorticoid regulation of Rev-erbalpha expression in liver, *Endocrinology* 141 (2000) 3799–3806.
- [24] G. Triqueneaux, S. Thenot, T. Kakizawa, M.P. Antoch, R. Safi, J.S. Takahashi, F. Delaunay, V. Laudet, The orphan receptor Rev-erbalpha gene is a target of the circadian clock pacemaker, *J. Mol. Endocrinol.* 33 (2004) 585–608.
- [25] G. Adelmant, A. Bègue, D. Stéhelin, V. Laudet, A functional Rev-erb alpha responsive element located in the human Rev-erb alpha promoter mediates a repressing activity, *Proc. Natl. Acad. Sci. U. S. A.* 93 (1996) 3553–3558.
- [26] R.W. Noyes, A.T. Hertig, J. Rock, Dating the endometrial biopsy, *Am. J. Obstet. Gynecol.* 122 (1975) 262–263.
- [27] Y. Osuga, H. Toyoshima, N. Mitsuhashi, Y. Taketani, The presence of platelet-derived endothelial cell growth factor in human endometrium and its characteristic expression during the menstrual cycle and early gestational period, *Hum. Reprod.* 10 (1995) 989–993.
- [28] K. Koga, Y. Osuga, O. Tsutsumi, T. Yano, O. Yoshino, Y. Takai, H. Matsumi, H. Hiroi, K. Kugu, M. Momoeda, T. Fujiwara, Y. Taketani, Demonstration of angiogenin in human endometrium and its enhanced expression in endometrial tissues in the secretory phase and the decidua, *J. Clin. Endocrinol. Metab.* 86 (2001) 5609–5614.
- [29] Y. Hirota, Y. Osuga, T. Hirata, O. Yoshino, K. Koga, M. Harada, C. Morimoto, E. Nose, T. Yano, O. Tsutsumi, Y. Taketani, Possible involvement of thrombin/protease-activated receptor 1 system in the pathogenesis of endometriosis, *J. Clin. Endocrinol. Metab.* 90 (2005) 3673–3679.
- [30] K. Hanley, L. Wood, D.C. Ng, S.S. He, P. Lau, A. Moser, P.M. Elias, D.D. Bikle, M.L. Williams, K.R. Feingold, Cholesterol sulfate stimulates involucrin transcription in keratinocytes by increasing Fra-1, Fra-2, and Jun D, *J. Lipid Res.* 42 (2001) 390–398.
- [31] C. Chauvet, B. Bois-Joyeux, J.L. Danan, Retinoic acid receptor-related orphan receptor (ROR) alpha4 is the predominant isoform of the nuclear receptor RORalpha in the liver and is up-regulated by hypoxia in HepG2 human hepatoma cells, *Biochem. J.* 364 (2002) 449–456.
- [32] T. Hirata, Y. Osuga, K. Hamasaki, Y. Hirota, E. Nose, C. Morimoto, M. Harada, Y. Takemura, K. Koga, O. Yoshino, T. Tajima, A. Hasegawa, T. Yano, Y. Taketani, Expression of toll-like receptors 2, 3, 4, and 9 genes in the human endometrium during the menstrual cycle, *J. Reprod. Immunol.* 74 (2007) 53–60.
- [33] M. Becker-André, E. André, J.F. DeLamar, Identification of nuclear receptor mRNAs by RT-PCR amplification of conserved zinc-finger motif sequences, *Biochem. Biophys. Res. Commun.* 194 (1993) 1371–1379.
- [34] P. Lau, Bailey, D.H. Dowhan, G.E. Muscat, Exogenous expression of a dominant negative RORalpha1 vector in muscle cells impairs differentiation: RORalpha1 directly interacts with p300 and myoD, *Nucleic Acids Res.* 27 (1999) 411–420.
- [35] E. Raspé, H. Duez, P. Gervois, C. Fiévet, J.C. Fruchart, S. Besnard, J. Mariani, A. Tedgui, B. Staels, Transcriptional regulation of apolipoprotein C-III gene expression by the orphan nuclear receptor RORalpha, *J. Biol. Chem.* 276 (2001) 2865–2871.
- [36] N. Vu-Dac, P. Gervois, T. Grötzinger, P. De Vos, K. Schoonjans, J.C. Fruchart, J. Auwerx, J. Mariani, A. Tedgui, B. Staels, Transcriptional regulation of apolipoprotein A-I gene expression by the nuclear receptor RORalpha, *J. Biol. Chem.* 272 (1997) 22401–22404.
- [37] P. Delerive, D. Monté, G. Dubois, F. Trottein, J. Fruchart-Najib, J. Mariani, J.C. Fruchart, B. Staels, The orphan nuclear receptor ROR alpha is a negative regulator of the inflammatory response, *EMBO Rep.* 2 (2001) 42–48.
- [38] B. Kopmels, J. Mariani, V. Taupin, N. Delhay-Bouchaud, E.E. Wollman, Differential IL-6 mRNA expression by stimulated peripheral macrophages of Staggerer and Lurcher cerebellar mutant mice, *Eur. Cytokine Netw.* 2 (1991) 345–353.
- [39] S. Besnard, J.S. Silvestre, M. Duriez, J. Bakouche, Y. Lemaigre-Dubreuil, J. Mariani, B.I. Levy, A. Tedgui, Increased ischemia-induced angiogenesis in the staggerer mouse, a mutant of the nuclear receptor RORalpha, *Circ. Res.* 89 (2001) 1205–1215.
- [40] J. Wang, L. Yin, M.A. Lazar, The orphan nuclear receptor Rev-erb alpha regulates circadian expression of plasminogen activator inhibitor type 1, *J. Biol. Chem.* 281 (2006) 33842–33848.
- [41] D.J. Kennaway, T.J. Varcoe, V.J. Mau, Rhythmic expression of clock and clock-controlled genes in the rat oviduct, *Mol. Hum. Reprod.* 9 (2003) 503–507.
- [42] J.A. Kallen, J.M. Schlaeppi, F. Bitsch, S. Geisse, M. Geiser, I. Delhon, B. Fournier, X-ray structure of the hRORalpha LBD at 1.63 Å: structural and functional data that cholesterol or a cholesterol derivative is the natural ligand of RORalpha, *Structure* 10 (2002) 1697–1707.
- [43] S. Balasubramaniam, A. Szanto, P.D. Roach, Circadian rhythm in hepatic low-density-lipoprotein (LDL)-receptor expression and plasma LDL levels, *Biochem. J.* 298 (1994) 39–43.